Inorg. Chem. **2005**, *44*, 6975–6982

Study of Hg_2^{2+} and Complexes of NpO_2^{+} and UO_2^{2+} in Solution. Examples of Cation–Cation Interactions

Michael L. McKee*,† and Marcel Swart‡

Department of Chemistry and Biochemistry, Auburn University, Auburn, Alabama 36849, and Organic and Inorganic Chemistry, Vrije Universiteit, De Boelelaan 1083, NL-1081 HV Amsterdam, The Netherlands

Received February 11, 2005

Density functional theory (BPW91/TZ2P) is used to explore the nature of cation–cation interactions (CCIs) that exist between two actinyl cations in solution. Solvation, which is modeled using COSMO, favors the complexes $(ONpO–ONpO)^{2+}$ and $(ONpO–OUO)^{3+}$ over separated NpO_2^{+}(aq) and UO_2^{2+}(aq) cations because of the quadratic dependence of solvation on charge. For $(OUO–OUO)^{4+}$, solvation effects, even though very large, are unable to overcome intrinsic electrostatic repulsion between the units. The actinyl–actinyl complexes are T-shaped, with the oxygen of one unit coordinated to the actinide metal of the other unit. The association free energies of $(ONpO–ONpO)^{2+}$ and $(ONpO–OUO)^{3+}$ are calculated as –42.1 and –29.2 kcal/mol. Explicit consideration of the first solvation shell at the B3LYP/LANL2DZ level suggests that the free energies of binding may be overestimated. The Hg_2^{2+} dication, though not considered a "traditional" CCI, is very similar to the actinyl–actinyl interaction. The binding free energy of Hg_2^{2+} in solution is calculated as –16.0 kcal/mol.

Introduction

Cation−cation interactions (CCIs) are generally considered as the interactions between an actinyl cation, AnO_2^{+} and AnO_2^{2+}, and another actinyl cation or "active" cations such as Th^{4+}, Cr^{3+}, Fe^{3+}, Ga^{3+}, Sc^{3+}, In^{3+}, Bi^{3+}, Pb^{2+}, Hg^{2+}, Hg^{+}, and Rh^{3+}.[1−15] These interactions have been observed in the solid state, in solution, and in melts. In solution, the complexes $(ONpO−ONpO)^{2+}$ and $(OUO−ONpO)^{3+}$ are well-characterized.[1,2] Complexes where both monomers have a charge greater than 1+ (such as $(OUO−OUO)^{4+}$) are unknown. In solution, the structure of the actinyl−actinyl complex, an association between ions of like charge,[16−18] is T-shaped.[1]

Calculations of elements in the actinide and lanthanide series require careful consideration because of strong relativistic and spin−orbit effects and closely spaced orbitals.[19−32]

* To whom correspondence should be addressed. E-mail: mckee@chem.auburn.edu.

† Auburn University.

‡ Vrije Universiteit.

(1) Krot, N. N.; Grigoriev, M. S. *Russ. Chem. Rev.* **2004**, *73*, 89.
(2) Stoyer, N. J.; Hoffman, D. C.; Silva, R. J. *Radiochim. Acta* **2000**, *88*, 279.
(3) Gregoire-Kappenstein, A. C.; Moisy, Ph.; Cote, G.; Blanc, P. *Radiochim. Acta* **2003**, *91*, 665.
(4) Auwer, C. D.; Grégoire-Kappenstein, A. C.; Moisy, Ph. *Radiochim. Acta* **2003**, *91*, 773.
(5) Barbanel', Yu. A.; Dushin, R. B.; Kolin, V. V.; Kotlin, V. P.; Mashirov, L. G.; Nekhoroshkov, S. N. *Radiochemistry* **2003**, *45*, 276.
(6) Sullens, T. A.; Jensen, R. A.; Shvareva, T. Y.; Albrecht-Schmitt, T. E. *J. Am. Chem. Soc.* **2004**, *126*, 2676.
(7) Albrecht-Schmitt, T. E.; Almond, P. M.; Sykora, R. E. *Inorg. Chem.* **2003**, *42*, 3788.
(8) Grigoriev, M. S.; Antipin, M. Yu.; Krot, N. N.; Garnov, A. Yu. *Radiochemistry* **2002**, *44*, 458.
(9) Madic, C.; Begun, G. M.; Hobart, D. E.; Hahn, R. L. *Inorg. Chem.* **1984**, *23*, 1914.
(10) Guillaume, B.; Hahn, R. L.; Narten, A. H. *Inorg. Chem.* **1983**, *22*, 109.
(11) Guillaume, B.; Begun, G. M.; Hahn, R. L. *Inorg. Chem.* **1982**, *21*, 1159.
(12) Murmann, R. K.; Sullivan, J. C. *Inorg. Chem.* **1967**, *6*, 892.
(13) Newton, T. W.; Baker, F. B. *Inorg. Chem.* **1965**, *4*, 1166.
(14) Sullivan, J. C. *Inorg. Chem.* **1964**, *3*, 315.
(15) Sullivan, J. C.; Hindman, J. C.; Zielen, A. J. *J. Am. Chem. Soc.* **1961**, *83*, 3373.
(16) Troxler, L.; Harrowfield, J. M.; Wipff, G. *J. Phys. Chem. A* **1998**, *102*, 6821.
(17) Jenkins, H. D. B.; Marcus, Y. *Chem. Rev.* **1995**, *95*, 2725.
(18) Marcus, Y. *Ion Solvation*; John Wiley: Chichester, U.K., 1985; p 306.
(19) Wang, S. G.; Pan, D. K.; Schwarz, W. H. E. *J. Chem. Phys.* **1995**, *102*, 9296.
(20) Schreckenbach, G.; Hay, P. J.; Martin, R. L. *J. Comput. Chem.* **1999**, *20*, 70.
(21) Hay, P. J.; Martin, R. L.; Schreckenbach, G. *J. Phys. Chem. A* **2000**, *104*, 6259.
(22) Straka, M.; Dyall, K. G.; Pyykkö, P. *Theor. Chem. Acc.* **2001**, *106*, 393.
(23) García-Hernández, M.; Lauterbach, C.; Krüger, S.; Matveev, A.; Rösch, N. *J. Comput. Chem.* **2002**, *23*, 834.
(24) Kaltsoyannis, N. *Chem. Soc. Rev.* **2003**, *32*, 9.

10.1021/ic050224o CCC: $30.25
Published on Web 09/08/2005

Nevertheless, theoretical results are sufficiently reliable to provide support and interpretation for experimentalists. In the following work, we will combine electronic structure calculations of dinuclear actinide complexes with a consideration of solvation to put the concept of CCIs on a firmer theoretical foundation. It will be shown that large solvation effects are required to overcome the inherent electrostatic repulsion. While the dinuclear mercury complex Hg_2^{2+} is not considered a CCI, the electronic/solvation description is very similar to that of the actinyl complexes.

Computational Details

Geometries were optimized at the density functional level[33] with the BPW91 exchange/correlation functionals[34] and a TZ2P basis set[35] with ADF[36] including scalar relativistic effects through the ZORA method.[37] The core electrons ([1s]O and [Xe]4f5d/Hg/Np/U) were treated with the frozen-core approximation,[34a] while a doubly polarized triple-ξ basis set was used for the oxygen (2s2p+df) and mercury/neptunium/uranium (6s6p|7s5f6d+pf) atoms, respectively. The gas-phase UO_2^{2+} cation has received extensive attention because of its stability and unambiguous closed-shell ground state.[21,23,31,38−44] We compare our results with a selection of high-level results from other studies in Table 1.

Table 1. Comparison of Calculated U−O Bond Lengths in UO_2^{2+}(g)

U−O (Å)	method/basis set	ref
1.702	CCSD(T)/U(RSC+2g) + O(aug-cc-pVDZ)	*a*
1.695	B3LYP/U(RSC+2g) + O(aug-cc-pVDZ)	*a*
1.713	BP/Stoll−Preuss ECP (small core)	*b*
1.721	BP/all-electron scalar relativistic	*b*
1.715	Dirac−Hartee−Fock/U(VTZ) + O(cc-pVTZ)	*c*
1.719	BPW91/TZ2P + ZORA	*d*

[a] Reference 31. [b] Reference 41. [c] Reference 42. [d] This work.

Table 2. Energies (kcal/mol) Optimized in the Gas Phase and in Solution (COSMO) at the BPW91/TZ2P Level

	state	gas phase	solution	Δ^a
Hg^+	^2S	0.0	−83.4	−83.4
Hg_2^{2+}	$^1\Sigma_g^+$	51.4	−195.3	−246.7
NpO_2^+	^3H_g	−539.0	−625.0	−86.0
UO_2^{2+}	$^1\Sigma_g^+$	−575.1	−899.0	−323.9
$(ONpO-ONpO)^{2+}$	$^5B_1$	−1022.1	−1300.0	−277.9
$(ONpO-OUO)^{3+}$	$^3B_2$	−1023.5	−1561.0[b]	−537.5
$(OUO-ONpO)^{3+}$	$^3B_1$	−1007.9	−1546.7	−538.8
$(OUO-OUO)^{4+}$	$^1A_1$	*c*	−1792.7	

[a] The difference between the gas-phase and solution energies is closely related to the solvation free energies. [b] The COSMO optimzation of $(ONpO-OUO)^{3+}$ did not meet all of the stopping criteria for the gradients. [c] No minimum was found for the $(OUO-OUO)^{4+}$ complex in the gas phase.

The C_{2v} point group was used for linear $ONpO^+/OUO^{2+}$ and the $ONpO^+/OUO^{2+}$ T-shaped complexes. Atomic charges were determined from an atomic multipole expansion.[45] Solvation effects were taken into account with COSMO, a conductor-like screening model implemented in ADF.[46] The following atomic radii were used in the COSMO calculations: 2.108, 2.100, 2.100, and 1.517 Å for Hg, Np, U, and O, respectively (MM3 values that have been scaled by 1/1.2).[47] A dielectric constant of 78.4 was used.

The structures of all species were optimized in the gas phase and in aqueous solution and are presented in Figure 1. The gas-phase and COSMO energies (relative to atomic reference atoms) for all species considered at the BPW91/TZ2P level are presented in Table 2.

Vibrational frequencies were not calculated by ADF for the actinyl complexes for technical reasons. While zero-point and heat capacity corrections are expected to be small, the effect of entropy on binding free energies will be more significant. To calculate the entropy effect and to estimate the effect of explicitly considering the first hydration shell of NpO_2^+ and UO_2^{2+} (i.e., $NpO_2(H_2O)_5^+$ and $UO_2(H_2O)_5^{2+}$), B3LYP/LANL2DZ optimizations and frequency calculations (B3LYP/SDD for mercury species) were made on all species (except $(OUO-OUO)^{4+}$) using Gaussian03[48] (Table 3). Continuum solvation effects at the B3LYP/LANL2DZ level were computed using a dielectric constant of 78.39 and the CPCM method.[49] The B3LYP/LANL2DZ (B3LYP/SDD level for mercury species) entropies were combined with BPW91/TZ2P binding energies to estimate gas-phase binding

(25) Dolg, M. Lanthanides and Actinides. In *Encyclopedia of Computational Chemistry*; Schleyer, P. v. R., Allinger, N. L., Clark, T., Gasteiger, J., Kollman, P. A., Schaefer, H. F., III, Schreiner, P. R., Eds.; Wiley: Chichester, U.K., 1998.
(26) Cao, X.; Dolg, M.; Stoll, H. *J. Chem. Phys.* **2003**, *118*, 487.
(27) Bursten, B. E.; Drummond, M. L.; Li, J. *Faraday Discuss.* **2003**, *124*, 1.
(28) Balasubramanian, K.; Siekhaus, W. J.; McLean, W., II. *J. Chem. Phys.* **2003**, *119*, 5889.
(29) Paulovič, J.; Nakajima, T.; Hirao, K.; Liondh, R.; Malmqvist, P. Å *J. Chem. Phys.* **2003**, *119*, 798.
(30) Han, J.; Kaledin, L. A.; Goncharov, V.; Komissarov, A. V.; Heaven, M. C. *J. Am. Chem. Soc.* **2003**, *125*, 7176.
(31) Straka, M.; Patzschke, M.; Pyykkö, P. *Theor. Chem. Acc.* **2003**, *109*, 332.
(32) For an online bibliography of relativistic quantum chemical studies, see: http://www.csc.fi/lul/rtam.
(33) Koch, W.; Holthausen, M. C. *A Chemist's Guide to Density Functional Theory*; Wiley: New York, 2001.
(34) (a) Perdew, J.; Wang, Y. *Phys. Rev. B* **1992**, *45*, 13244. (b) Becke, A. D. *Phys. Rev. A* **1988**, *38*, 3098.
(35) Van Lenthe, E.; Baerends, E. J. *J. Comput. Chem.* **2003**, *24*, 1142.
(36) (a) te Velde, G.; Bickelhaupt, F. M.; van Gisbergen, S. J. A.; Fonseca Guerra, C.; Baerends, E. J.; Snijders, J. G.; Ziegler, T. Chemistry with ADF. *J. Comput. Chem.* **2001**, *22*, 931. (b) Fonseca Guerra, C.; Snijders, J. G.; te Velde, G.; Baerends, E. J. *Theor. Chem. Acc.* **1998**, *99*, 391. (c) ADF2002.03, SCM, Theoretical Chemistry, Vrije Universiteit, Amsterdam, The Netherlands, http://www.scm.com.
(37) (a) van Lenthe, E.; Ehlers, A. E.; Baerends, E. J. *J. Chem. Phys.* **1999**, *110*, 8943. (b) van Lenthe, E.; Baerends, E. J.; Snijders, J. G. *J. Chem. Phys.* **1994**, *101*, 9783. (c) van Lenthe, E.; Snijders, J. G.; Baerends, E. J. *J. Chem. Phys.* **1996**, *105*, 6505. (d) van Lenthe, E.; et al. *Int. J. Quantum Chem.* **1996**, *57*, 281.
(38) Vallet, V.; Privalov, T.; Wahlgren, U.; Grenthe, I. *J. Am. Chem. Soc.* **2004**, *126*, 7766.
(39) Clark, A. E.; Sonnenberg, J. L.; Hay, P. J.; Martin, R. L. *J. Chem. Phys.* **2004**, *121*, 2563.
(40) Clavaguéra-Sarrio, C.; Vallet, V.; Maynau, D.; Marsden, C. J. *J. Chem. Phys.* **2004**, *121*, 5312.
(41) Moskaleva, L. V.; Krüger, S.; Spörl, A.; Rösch, N. *Inorg. Chem.* **2004**, *43*, 4080.
(42) de Jong, W. A.; Harrison, R. J.; Nichols, J. A.; Dixon, D. A. *Theor. Chem. Acc.* **2001**, *107*, 22.
(43) Majumdar, D.; Balasubramanian, K.; Nitsche, H. *Chem. Phys. Lett.* **2002**, *361*, 143.
(44) Toraishi, T.; Privalov, T.; Schimmelpfennig, B.; Wahlgren, U.; Grenthe, I. *J. Phys. Chem. A* **2003**, *107*, 9456.
(45) Swart, M.; Van Duijnen, P. Th.; Snijders, J. G. *J. Comput. Chem.* **2001**, *22*, 79.
(46) Pye, C. C.; Ziegler, T. *Theor. Chem. Acc.* **1999**, *101*, 396.
(47) (a) Because MM2/MM3 radii are generally 20−30% larger than the usual van der Waals radii for a number of "organic" atoms (H, C, N, O, S, F, etc.),[47b] we use the MM2 radii with a 1/1.2 (0.8333) scaling factor. (b) Allinger, N. L.; Zhou, X.; Bergsma, J. *THEOCHEM* **1994**, *312*, 69.

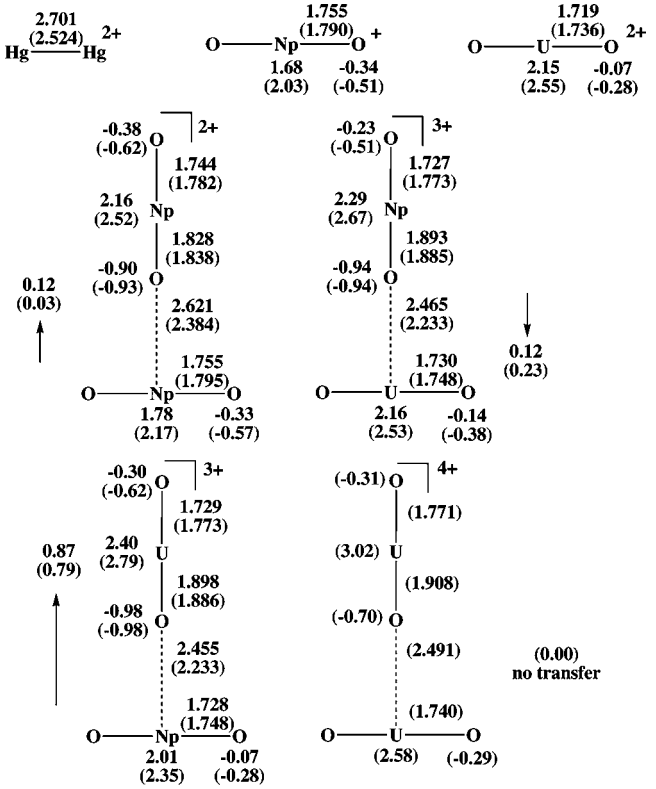

Figure 1. Optimized geometries of species at the BPW91/TZ2P level in the gas phase and in solution. Geometric distances (Å) are given on the right-hand side of the structure, and multipole charges are given on the left-hand side. In parentheses are values for the COSMO-optimized structures. An arrow indicates the direction and amount of charge transfer from one actinyl unit to another.

free energies (Table 4). The last column in Table 4 (COSMO-TΔS) refers to our best estimate of aqueous-phase binding free energies.

Result and Discussion

The discussion will be divided into a section on the Hg_2^{2+} complex and one on the actinyl complexes.

Hg_2^{2+}. While two Hg^+ cations with $6s^1$ configuration can form a σ bond, the strength of the bond is less than the electrostatic repulsion. Durand et al.[50] used a relativistic ECP to describe the core electrons and a (5s,5p,2d) basis contracted to [3s,4p,2d] to describe the 6s/5d valence electrons. When spin−orbit effects are taken into account, the Hg_2^{2+} $^1\Sigma_g$ ground state is a local minimum about 60 kcal/mol above the $Hg^+(^2S) + Hg^+(^2S)$ asymptote. Neisler and Pitzer[51] used a relativistic effective core potential with a double-ζ s,p,d basis set of Slater-type functions to compute Hg_2^{2+}. With CI and including spin−orbit effects (REP CI), they calculated the complex to be a local minimum with a Hg−Hg separation of 2.54 Å (182 ω_e/cm^{-1}) and 26 kcal/mol above two Hg^+ cations.

While the Hg_2^{2+} complex is predicted to be a minimum in the gas phase, the search for the dication complex has, to date, been unsuccessful.[52] In contrast, the aqueous chemistry of Hg_2^{2+} is well-established.[53,54] The equilibrium constant (298 K) for the disproportionation reaction, eq 1, is $K = [Hg^{2+}]/[Hg_2^{2+}] = 1.14 \times 10^{-2}$.[54] Because disproportionation

$$Hg_2^{2+}(aq) \rightleftarrows Hg^{2+}(aq) + Hg(l) \quad (1)$$

$$Hg_2^{2+}(aq) \rightleftarrows 2Hg^{+}(aq) \quad (2)$$

(eq 1) occurs before dissociation (eq 2), the dissociation reaction (eq 2) must have a free energy of reaction greater than 2.6 kcal/mol at 298 K in aqueous solution.

The calculated Hg−Hg distance of Hg_2^{2+} in the gas phase is 2.701 Å (116.7 ω_e/cm^{-1}), and the binding energy is −51.4 kcal/mol (i.e., unbound). In solution, the COSMO binding energy is 28.4 kcal/mol. Thus, the thermodynamic stability of Hg_2^{2+} is entirely due to solvation. In the gas → solution transition, the calculated Hg−Hg distance decreases by 0.177 Å to a value of 2.524 Å while the calculated stretching frequency increases from 116.7 to 154.8 cm^{-1}. The Hg−Hg distance of Hg_2^{2+} in solution is known from EXAFS studies[55] to be 2.52 Å with a stretching frequency of 171.5 cm^{-1}.

The free energies of solvation of Hg^+ and Hg_2^{2+} are calculated to be 83.4 and 246.6 kcal/mol, respectively (Table 2), but no experimental values are available for comparison.

Table 3. Total Energies (Hartrees), Zero-Point Energies (kcal/mol), Heat Capacity Corrections to 298 K (kcal/mol), Entropies (cal/mol·K), Solvation Free Energies (kcal/mol) in Water ($\epsilon = 78.39$) at the CPCM/B3LYP/LANL2DZ Level, and Nonelectrostatic Contribution to the Solvation Free Energies (kcal/mol) for Geometries Optimized at the B3LYP/LANL2DZ Level

	point group/state	B3LYP/LANL2DZ	ZPE(NIF)[b]	Cp Corr	entropy	ΔG(solv)	nonelec
Hg^{+} [a]	$K/^2S$	−153.191 72	0.00	1.48	53.68[c]	−186.80	3.18
Hg_2^{2+} [a]	$D_{\infty h}/^1\Sigma_g^+$	−306.278 73	0.17(0)	2.51	65.79	−457.47	6.36
H_2O	$C_{2v}/^1A_1$	−76.414 32	13.02(0)	2.38	45.13	−11.20	2.25
$ONpO^+$	$D_{\infty h}/^3X$[d]	−211.283 35	3.11(0)	2.83	63.98	−202.91	6.16
OUO^{2+}	$D_{\infty h}/^1\Sigma_g^+$	−201.203 96	3.22(0)	2.99	63.71	−461.97	5.99
$(ONpO-ONpO)^{2+}$	$C_{2v}/^5A_1$	−422.492 32[e]	6.40(1)	5.37	101.58	−459.34	12.00
$(ONpO-OUO)^{3+}$	$C_{2v}/^3B_2$	−412.362 20	6.62(0)	5.82	101.47	−746.03	11.54
$(OUO-ONpO)^{3+}$	$C_{2v}/^3B_2$	−412.332 88	6.34(0)	5.23	96.33	−749.19	11.53
$NpO_2(H_2O)_5^+$	$D_5/^3X$[d]	−593.624 90[f]	78.77(2)	11.86	137.01	−90.01	10.89
$OUO_2(H_2O)_5^{2+}$	$D_5/^1A_1$	−583.747 30	82.32(0)	11.21	127.99	−211.42	9.75
$(ONpO(H_2O)_5-ONpO(H_2O)_4)^{2+}$	$C_s/^5A'$	−1110.777 56[g]	146.12(2)	21.10	216.41	−203.27	20.98
$(ONpO(H_2O)_5-OUO(H_2O)_4)^{3+}$	$C_s/^3A''$	−1100.829 57[h]	148.72(2)	20.15	204.63	−368.01	20.28
$(OUO(H_2O)_5-ONpO(H_2O)_4)^{3+}$	$C_s/^3A''$	−1100.806 09[i]	148.76(3)	19.52	195.34	−369.01	20.02

[a] Values for mercury species are at the B3LYP/SDD level. [b] The number of imaginary frequencies is given in parentheses. [c] From the NIST Standard Reference Database. http://webbook.nist.gov/chemistry. [d] Mixed electronic state. [e] Reducing the symmetry to C_1 did not lead to a lower energy. [f] The optimized C_1 symmetry structure is 0.08 kcal/mol lower in energy. [g] The optimized C_1 symmetry structure is 0.11 kcal/mol lower in energy. [h] The optimized C_1 symmetry structure is 0.05 kcal/mol lower in energy. [i] The optimized C_1 symmetry structure is 1.84 kcal/mol lower in energy.

Table 4. Gas-Phase and Solution (COSMO) Reaction Energies (kcal/mol) and Best Estimates of Solution Reaction Free Energies

	relative energies		effect of solvation solution	ΔG(aq) estimate[a] COSMO − $T\Delta S$
	gas	solution		
$2Hg^{+} \rightarrow Hg_2^{2+}$	51.4	−28.4	−79.8	−16.0
$2NpO_2^{+} \rightarrow (ONpO-ONpO)^{2+}$	55.9	−50.0	−105.8	−42.1
$NpO_2^{+} + UO_2^{2+} \rightarrow (ONpO-OUO)^{3+}$	90.5	−37.0	−127.5	−29.2
$NpO_2^{+} + UO_2^{2+} \rightarrow (OUO-ONpO)^{3+}$	106.1	−22.6	−128.7	−13.3
$2UO_2^{2+} \rightarrow (OUO-OUO)^{4+}$	*c*	5.3		13.2[b]

[a] The $T\Delta S$ contribution calculated at the B3LYP/SDD or B3LYP/LANL2DZ level (Table 3) is subtracted from the COSMO relative energies. [b] The entropy of reaction is assumed to be the same as that of $NpO_2^{+} + UO_2^{2+} \rightarrow (ONpO-OUO)^{3+}$. [c] No minimum was found for the $(OUO-OUO)^{4+}$ complex in the gas phase.

However, an estimate can be made with the experimental data[56] from Table 5 and the calculated gas-phase dissociation energy of Hg_2^{2+} (Table 2).

$$2Hg(g) \rightarrow 2Hg^{+}(g) \quad (3a)$$

$$2Hg^{+}(g) \rightarrow Hg_2^{2+}(g) \quad (3b)$$

$$Hg_2^{2+}(g) \rightarrow Hg_2^{2+}(aq) \quad (3c)$$

The entropy of the association equation 3b was calculated to be 41.57 cal/mol·K at the B3LYP/SDD level (Table 3) and used to estimate the gas-phase free-energy change of eq 3b as 63.8 kcal/mol at 298 K. The estimated free energy of solvation of eq 3c (−310.5 kcal/mol) can be

$$\Delta G = \text{eq 3a} + \text{eq 3b} + \text{eq 3c} \quad (4a)$$

$$\Delta G = 469.2 + 63.8 + x = 222.6 \text{ kcal/mol} \quad (4b)$$

$$x = -310.5 \text{ kcal/mol} \quad (4c)$$

compared with the COSMO value of −246.6 kcal/mol (Table 2). The solvation free energy of Hg^{+} is not known but can be estimated as one-fourth of the free energy of solvation of Hg^{2+} (−443.5 kcal/mol) because of the quadratic dependence of solvation on the ionic charge.[57] The value determined in this way is −110.9 kcal/mol, which can be compared to the COSMO value of −83.4 kcal/mol (Table 2). The COSMO solvation free energies may be too small but could easily be increased by simply changing the ionic radius. However, the errors largely cancel when relative solvation free energies are compared. Thus, the free-energy change of eq 5 is 24.9 kcal/mol estimated using experimental data and 16.0 kcal/mol by COSMO (Table 4). Both values are larger than 2.6 kcal/mol, which is consistent with the observed disproportionation (eq 1) rather than dissociation (eq 2) of Hg_2^{2+}(aq).

Table 5. Experimental Thermodynamic Data for Mercury[a]

	ΔH(298 K)	ΔS(298 K)	ΔG(298 K) absolute thermochemical scale[b]	ΔG(298 K) conventional thermochemical scale
Hg(l)	0.0	18.2	0.0	0.0
Hg(g)	14.7	41.8[c]	7.6	7.6
Hg^{+}(g)	256.8	53.7[c]	242.2	141.7
Hg^{+}(aq)			(131.4)[d]	(30.8)[d]
Hg^{2+}(g)	690.8	41.8	683.9	482.9
Hg^{2+}(aq)	40.7		240.4	39.4
Hg_2^{2+}(g)		[65.8][e]		
Hg_2^{2+}(aq)	39.9		237.8	36.7

[a] Thermal electron standard state. Unless otherwise noted, data are taken from ref 56. [b] The correction to the absolute thermochemistry scale (H^{+}(aq) + e^{-}(g) → $^1/_2H_2$(g)) is ΔG = 100.5 kcal/mol. [c] From the NIST Standard Reference Database. http://webbook.nist.gov/chemistry. [d] The free energy assuming solvation free energy of Hg^{+} is 0.25(−443.5) = −110.9 kcal/mol of Hg^{2+}. [e] Calculated at the B3LYP/SDD level. See Table 3.

NpO_2^{+} and UO_2^{2+} Complexes. CCIs in the solid state and in solution have been reviewed by Krot and Grigoriev.[1] The weight of evidence suggests that the interaction in solution is inner sphere rather than outer sphere, where a water atom is displaced by an oxygen atom (Figure 2). There are five strongly coordinating water molecules in $[NpO_2(H_2O)_5]^{+}$ and $[UO_2(H_2O)_5]^{2+}$.[58] Upon formation of a cation−cation complex, a coordinated water is lost from the first

(48) Frisch, M. J.; Trucks, G. W.; Schlegel, H. B.; Scuseria, G. E.; Robb, M. A.; Cheeseman, J. R.; Montgomery, J. A., Jr.; Vreven, T.; Kudin, K. N.; Burant, J. C.; Millam, J. M.; Iyengar, S. S.; Tomasi, J.; Barone, V.; Mennucci, B.; Cossi, M.; Scalmani, G.; Rega, N.; Petersson, G. A.; Nakatsuji, H.; Hada, M.; Ehara, M.; Toyota, K.; Fukuda, R.; Hasegawa, J.; Ishida, M.; Nakajima, T.; Honda, Y.; Kitao, O.; Nakai, H.; Klene, M.; Li, X.; Knox, J. E.; Hratchian, H. P.; Cross, J. B.; Bakken, V.; Adamo, C.; Jaramillo, J.; Gomperts, R.; Stratmann, R. E.; Yazyev, O.; Austin, A. J.; Cammi, R.; Pomelli, C.; Ochterski, J. W.; Ayala, P. Y.; Morokuma, K.; Voth, G. A.; Salvador, P.; Dannenberg, J. J.; Zakrzewski, V. G.; Dapprich, S.; Daniels, A. D.; Strain, M. C.; Farkas, O.; Malick, D. K.; Rabuck, A. D.; Raghavachari, K.; Foresman, J. B.; Ortiz, J. V.; Cui, Q.; Baboul, A. G.; Clifford, S.; Cioslowski, J.; Stefanov, B. B.; Liu, G.; Liashenko, A.; Piskorz, P.; Komaromi, I.; Martin, R. L.; Fox, D. J.; Keith, T.; Al-Laham, M. A.; Peng, C. Y.; Nanayakkara, A.; Challacombe, M.; Gill, P. M. W.; Johnson, B.; Chen, W.; Wong, M. W.; Gonzalez, C.; Pople, J. A. *Gaussian 03*, revision B.4; Gaussian, Inc.: Wallingford, CT, 2004.

(49) CPCM is a conductor-like screening solvation model with a continuum polarizable description of solvent that takes into account both electrostatic and van der Waals contributions. (a) Cossi, M.; Scalmani, G.; Rega, N.; Barone, V. *J. Chem. Phys.* **2002**, *117*, 43. (b) Barone, V.; Cossi, M. *J. Phys. Chem. A* **1998**, *102*, 1995. (c) Barone, B.; Cossi, M.; Tomasi, J. *J. Comput. Chem.* **1998**, *19*, 404. (d) Takano, Y.; Houk, K. N. *J. Chem. Theory Comput.* **2005**, *1*, 70.

(50) Durand, G.; Spiegelmann, F.; Bernier, A. *J. Phys. B: At. Mol. Phys.* **1987**, *20*, 1161.

(51) Neisler, R. P.; Pitzer, K. S. *J. Phys. Chem.* **1987**, *91*, 1084.

(52) Curtis, J. M.; Boyd, R. K. *Rapid Commun. Mass Spectrom.* **1993**, *7*, 409.

(53) (a) Raposo, R. R.; Meléndez-Hevia, E.; Spiro, M. *J. Mol. Catal. A: Chem.* **2000**, *164*, 49. (b) Horváth, O.; Mikó, I. *J. Photochem. Photobiol. A* **1999**, *128*, 33. (c) Horváth, O.; Mikó, I. *Inorg. Chem. Commun.* **1999**, *2*, 143. (d) Autschbach, J.; Igna, C. D.; Ziegler, T. *J. Am. Chem. Soc.* **2003**, *125*, 4937. (e) Kaupp, M.; von Schnering, H. G. *Inorg. Chem.* **1994**, *33*, 4179.

(54) *Advanced Inorganic Chemistry*; Cotton, F. A., Wilkinson, G., Eds.; John Wiley: New York, 1988; pp 597−622.

(55) Rosdahl, J.; Persson, I.; Kloo, L.; Ståhl, K. *Inorg. Chim. Acta* **2004**, *357*, 2624.

(56) Hepler, L. G.; Olofsson, G. *Chem. Rev.* **1975**, *75*, 585.

(57) Fawcett, W. R. *J. Phys. Chem. B* **1999**, *103*, 11181.

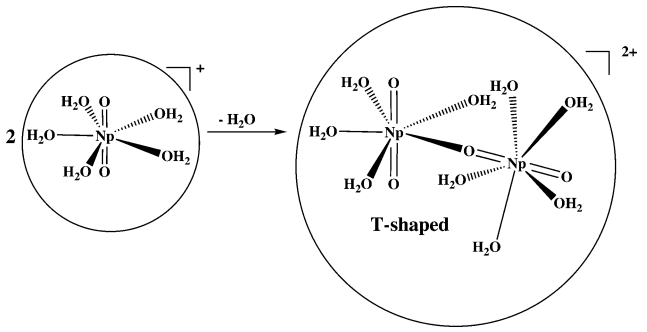

Figure 2. Depiction of CCI between two solvated NpO_2^{+} cations.

coordination sphere and replaced by an oxygen of the second actinyl unit. The existence of two cations in the same complex will increase the intracomplex electrostatic repulsion. However, because the complex has a greater positive charge, solvation effects are also expected to be greater (Figure 2). If the additional solvation is larger than the thermodynamic instability of the complex, a cation−cation complex will result. This is the case for Hg_2^{2+}, $(ONpO-ONpO)^{2+}$, and $(ONpO-OUO)^{3+}$ in solution but not for $(OUO-OUO)^{4+}$.

In the gas phase, a minimum is located for the T-shaped complexes $(ONpO-ONpO)^{2+}$, $(ONpO-OUO)^{3+}$, and $(OUO-ONpO)^{3+}$ (Figure 1). However, for the $(OUO-OUO)^{4+}$ complex, electrostatic replusion is too great for even a local minimum to exist in the gas phase. While the complexes are much less stable than separated actinyl units in the gas phase, COSMO predicts that the complexes will have much greater solvation free energy than the sum of the actinyl units and predicts all of the complexes to be bound except $(OUO-OUO)^{4+}$ (Table 4). Experimentally, there is no evidence for a UO_2^{2+}/UO_2^{2+} CCI in solution, but there is one example in the solid state.[6]

The experimental K_{eq} values for NpO_2^{+}/NpO_2^{+} and NpO_2^{+}/UO_2^{2+} are 0.7−3.7 and 0.8−1.4 M^{-1},[2] respectively, which suggest that the binding free energy must be very small. Because the calculated binding free energies of NpO_2^{+}/NpO_2^{+} and NpO_2^{+}/UO_2^{2+} are 42.1 and 29.2 kcal/mol, respectively (Table 4), the calculated binding free energy must be overestimated by about 30−40 kcal/mol. The COSMO method is a continuum method and may underestimate solvation when strong solvent−solute interactions occur. In the reaction $NpO_2^{+} + NpO_2^{2+} \rightarrow (ONpO-ONpO)^{3+}$, 10 strong water−actinide interactions are modeled by COSMO on the reactant side but only 9 on the product side (Figure 2). Thus, if the solvation energies are underestimated, cancellation of error will be incomplete and complexation energies will be overestimated. Water is tighly coordinated to UO_2^{2+}. Computationally, the binding enthalpy of H_2O in the $[UO_2(H_2O)_5]^{2+}$ complex is 65.8 kcal/mol.[38] In the $[UO_2(H_2O)_5]^{+}$ complex (which should be similar to $[NpO_2(H_2O)_5]^{+}$), the calculated binding enthalpy is reduced to 27.0 kcal/mol.[38]

To estimate the effect of explicitly including water molecules, calculations were carried out at the B3LYP/LANL2DZ level for NpO_2^{+}/UO_2^{2+} and $NpO_2(H_2O)_5^{+}/UO_2(H_2O)_5^{2+}$ with solvation effects included with the CPCM method (Figure 3 and Table 6). The B3LYP/LANL2DZ-optimized structures of NpO_2^{+} and UO_2^{2+} (Figure 3) are in reasonable agreement with the gas-phase geometries computed at the BPW91/TZ2P level including relativistic effects (Figure 1). In addition, the optimized structures of $NpO_2(H_2O)_5^{+}$ and $UO_2(H_2O)_5^{2+}$ (Figure 3) are in reasonable agreement with the solution-phase geometries of NpO_2^{+} and UO_2^{2+} computed at the BPW91/TZ2P level (Figure 1). The D_5 structure of $NpO_2(H_2O)_5^{+}$ had two imaginary frequencies at the B3LYP/LANL2DZ (Table 3) level but was only 0.1 kcal/mol less stable than the C_1-optimized structure. The most interesting feature of the explicitly solvated complexes (e.g., $(ONpO(H_2O)_5-ONpO(H_2O)_4)^{2+}$, etc.) was an internal hydrogen bond between one coordinated water and the oxygen atom of the actinyl unit. It is not clear whether the internal hydrogen-bonded structure would exist in solution because the coordinated water would compete with solvent for hydrogen bonding with the actinyl oxygen atom.

In a comparison of the B3LYP/LANL2DZ gas-phase $(ONpO-ONpO)^{2+}$ and $(ONpO(H_2O)_5-ONp(H_2O)_4)^{2+}$ complexes with COSMO-optimized BPW91/TZ2P structures, there is reasonable consistency in the bond length changes in going from the gas phase to solution. The degree of response in the bond lengths on going from $(ONpO-ONpO)^{2+}$ to $(ONpO(H_2O)_5-ONpO(H_2O)_4)^{2+}$ at the B3LYP/LANL2DZ level is greater than that on going from $(ONpO-ONpO)^{2+}$ in the gas phase to solution at the BPW91/TZ2P level. For example, the O−Np distance of the coordinated NpO_2^{+} increases 13% at B3LYP/LANL2DZ but only 9% at BPW91/TZ2P, while the proximal Np−O bond length within the coordinated NpO_2^{+} ligand increases 4% at B3LYP/LANL2DZ but only 1% at BPW91/TZ2P.

The predicted association of the actinyl cations is less favored at the B3LYP/LANL2DZ level compared to the BPW91/TZ2P level (Tables 4 and 6). In addition, explicit consideration of coordinated water reduces the free energy of binding by 12.0 kcal/mol for the NpO_2^{+}/NpO_2^{+} complex and 8.7 or 8.4 kcal/mol for the NpO_2^{+}/UO_2^{2+} complexes. If the free-energy difference from explicit consideration of coordinated water at the B3LYP/LANL2DZ level is added to the free energy of association determined at the BPW91/TZ2P level, the complexes are still predicted to be bound.

The solvation free energy of UO_2^{2+} has been studied theoretically by Moskaleva et al.[41] They found that both the continuum method (COSMO) and explicit consideration of the first hydration sphere (i.e., $UO_2(H_2O)_5^{2+}$) underestimated the solvation free energy of UO_2^{2+}, while a combination of both methods (using COSMO on the $UO_2(H_2O)_5^{2+}$ complex) overestimated the solvation free energy. Their best estimate (correcting for the expected error of the model) for ΔG(solv)

(58) (a) From X-ray scattering of UO_2^{2+} in an aqueous solution, the $UO_2(H_2O)_5^{2+}$ species is found to be dominant. See: Neuefeind, J.; Soderholm, L.; Skanthakumar, S. *J. Chem. Phys. A* **2004**, *108*, 2733. (b) From electrospray ionization of UO_2^{2+} in a water/acetone solution, the $[UO_2(CH_3COCH_3)_5]^{2+}$ species is detected. See: Van Stipdonk, M. J.; Chien, W.; Anbalagan, V.; Bulleigh, K.; Hanna, D.; Groenewold, G. S. *J. Phys. Chem. A* **2004**, *108*, 10448.

(59) Gagliardi, L.; Roos, B. O. *Inorg. Chem.* **2002**, *41*, 1315.

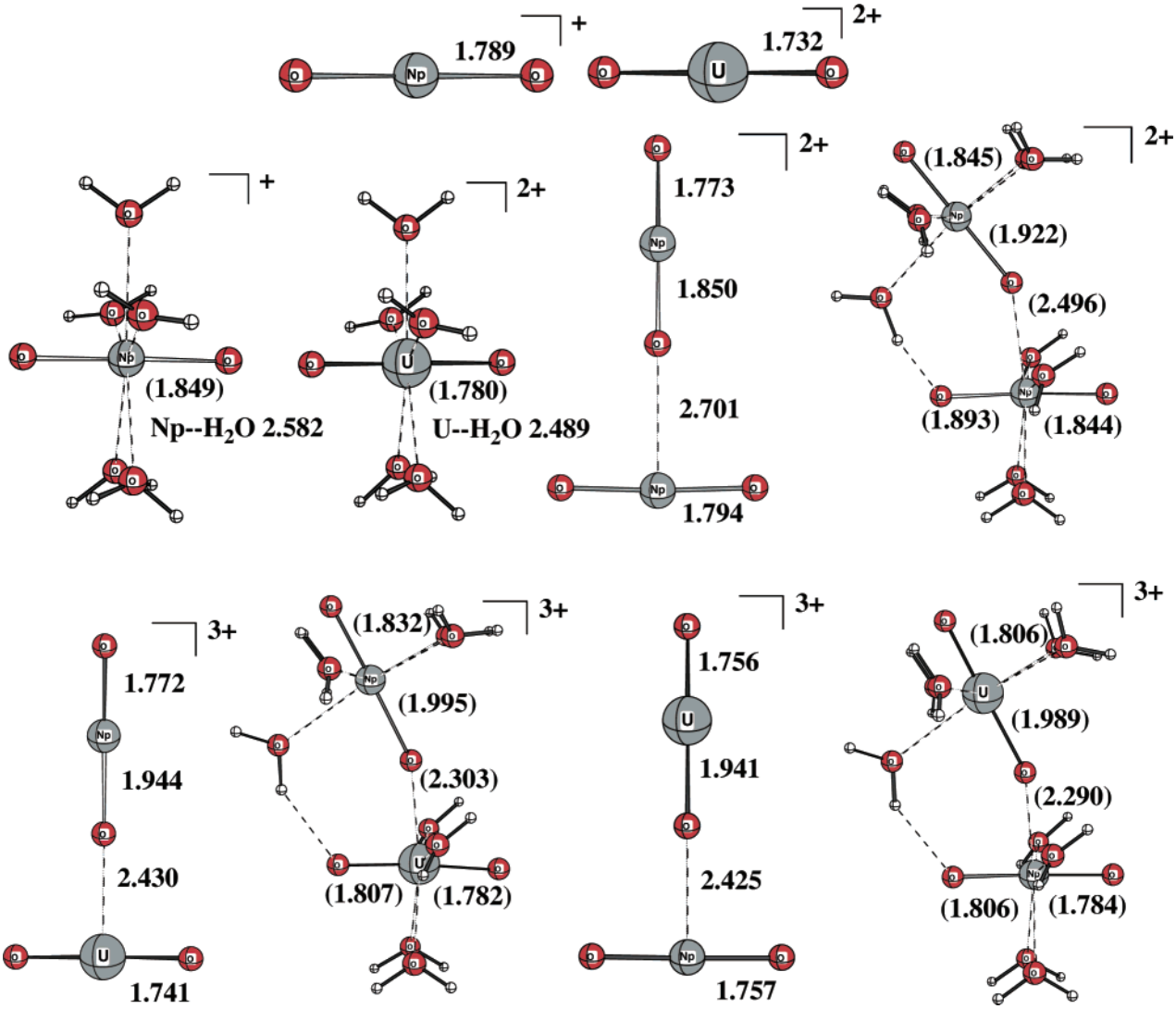

Figure 3. Optimized geometry of species at the B3LYP/LANL2DZ level.

Table 6. Reaction Enthalpies and Free Energies (kca/mol) in the Gas Phase and in Solution Calculated at the B3LYP/LANL2DZ Level (B3LYP/SSD for Mercury)

reactants → products	ΔH(0 K)	ΔH(298 K)	ΔG(g,298 K)	ΔG(aq,298 K)[a]	ΔG(aq,298 K)[b] corrected
$Hg^+ + Hg^+ \rightarrow Hg_2^{2+}$	65.9	65.5	77.9	−6.0	−7.9
$OUO^{2+} + 5H_2O \rightarrow UO_2(H_2O)_5^{2+}$	−282.0	−278.3	−237.6	61.5	40.1
$ONpO^+ + 5H_2O \rightarrow NpO_2(H_2O)_5^+$	−158.8	−161.7	−116.2	46.2	24.8
$ONpO^+ + ONpO^+ \rightarrow (ONpO-ONpO)^{2+}$	46.9	46.6	54.5	0.7	−1.2
$OUO^{2+} + ONpO^+ \rightarrow (ONpO-OUO)^{3+}$	78.8	78.8	86.6	4.9	3.0
$OUO^{2+} + ONpO^+ \rightarrow (OUO-ONpO)^{3+}$	96.9	96.3	105.6	20.7	18.8
$NpO_2(H_2O)_5^+ + NpO_2(H_2O)_5^+ \rightarrow (ONpO(H_2O)_5-ONpO(H_2O)_4)^{2+} + H_2O$	37.9	37.7	41.4	8.4	10.8
$UO_2(H_2O)_5^{2+} + NpO_2(H_2O)_5^+ \rightarrow (ONpO(H_2O)_5-OUO(H_2O)_4)^{3+} + H_2O$	81.2	80.7	85.2	9.3	11.7
$UO_2(H_2O)_5^{2+} + NpO_2(H_2O)_5^+ \rightarrow (OUO(H_2O)_5-ONpO(H_2O)_4)^{3+} + H_2O$	95.9	94.7	102.0	24.8	27.2

[a] ΔG(aq,298 K) = ΔG(g,298 K) + ΔG(solv) + nonelectrostatic term. [b] A correction of 1.9 kcal/mol is added to each species to account for the change of standard state from the gas phase (1 atm) to solution (1 M). An additional 2.4 kcal/mol correction is added to each free H_2O in the reaction to account for the change of state from solution (1 M) to liquid water (55.5 M).

was −370 kcal/mol.[60] Our value of −324.0 kcal/mol using COSMO (Table 2) is in fair agreement but somewhat too small for that expected for a continuum method.

Using wide-angle X-ray scattering, Guillaume et al.[10] have determined the Ac···Ac separation in $(ONpO-ONpO)^{2+}$ and $(ONpO-OUO)^{3+}$ as 4.2 Å. More recently, Auwer et al.[4] used EXAFS to determine the Np···Np separation in $(ONpO-ONpO)^{2+}$ as either 4.00 or 4.20 Å depending on the refining model. Our calculated Ac···Ac separations in solution in $(ONpO-ONpO)^{2+}$, $(ONpO-OUO)^{3+}$, and $(OUO-OUO)^{4+}$

(60) (a) A value of −397.9 kcal/mol has been reported[60b] for $\Delta H_{hyd}[UO_2^{2+}]$, which can be converted to ΔG(solv) = −369.4 kcal/mol for UO_2^{2+} using the entropy. (b) Gibson, J. K.; Haire, R. G.; Santos, M.; Marçalo, J.; Pires de Matos, A. *J. Phys. Chem. A* **2005**, *109*, 2768.

Table 7. Calculated Charges (e^-) in UO_2^{2+}

	charge				
	PCM[a] UO_2^{2+}(aq)	PCM[a] $UO_2(H_2O)_5^{2+}$(aq)	CPCM[b] $UO_2(H_2O)_5^{2+}$(aq)	COSMO[c,d] UO_2^{2+}(aq)	gas phase[c] UO_2^{2+}(g)
U/O	2.43/−0.21	2.43/−0.43[e]	2.29/−0.60[e]	2.55/−0.28	2.15/−0.07

[a] Mulliken atomic charges. Reference 38. [b] Mulliken atomic charges (B3LYP/U,O = (8s7p6d4f/2s3p2d)). Reference 61b. [c] Mulipole expansion charges. Reference 45. [d] This work. [e] The summed charges do not equal 2+ because some charge transfer to the coordinated water ligands has occurred.

are 4.222, 4.118, and 4.399 Å, respectively. The (OUO−OUO)$^{4+}$ cation complex is not known in solution, but a distance of 4.208 Å has been measured in a related X-ray structure.[6]

Our calculated electronic state of NpO_2^{+} has one 5fδ and one 5fϕ unpaired electron, which corresponds to a ^{3}H state, in agreement with previous calculations.[21,59] The Np−O distance increases from 1.755 to 1.790 Å when solvation is included, while in UO_2^{2+}, the U−O distance increases from 1.719 to 1.737 Å. The experimental (XAFS)[61,62] Np−O and U−O bond lengths of NpO_2^{+} and UO_2^{2+} in solution are 1.83 and 1.76 Å, respectively. Thus, the Np−O and U−O bond length increases in response to solvation are underestimated by the COSMO continuum solvation model.

The degree of charge polarization within the actinyl unit and charge transfer between actinyl units may be an important factor leading to observable cation−cation complexes in aqueous solution. For that reason, we compare multipole-expansion charges computed for UO_2^{2+} in the gas phase and solution with Mulliken charges by Vallet et al.[38] in Table 7. Clark et al.[39] have pointed out that Mulliken populations are unreliable for the actinyls. The solution-phase Mulliken charge by Vallet et al. for $[UO_2{\cdot}5H_2O]^{2+}$ indicates that 0.43 electrons have been transferred to the five coordinated water ligands. In our COSMO results (continuum model), charge transfer to coordinated ligands is not possible. There is a significant increase in the polarity of the U−O bonds in going from the gas phase to solution.

In the (ONpO−ONpO)$^{2+}$ T-shaped complex (Figure 1), the O−Np distance of the actinyl ligand has significantly increased and the charge on the oxygen atom coordinated to Np is much more negative compared to an oxygen atom in an uncoordinated NpO_2^{+} unit. There is evidence of typical donation/backdonation between Np and oxygen (Figure 4). In the gas phase, 0.12 e^- is transferred to the actinyl ligand, which is reduced to 0.03 e^- in solution. The dominant charge-transfer interaction is the overlap of the singly occupied Np f_{z^2x} orbital with the π^* Np═O bond.

In the mixed complex (ONpO−OUO)$^{3+}$, NpO_2^{+} is the ligand and U the metal center. There is significant charge donation (0.12 e^-, gas phase; 0.23 e^-, solution) from the O $2p_x$ atomic orbital of the π Np═O bond into the empty U f_{z^2x} orbital. As well, there is significant lengthening of the

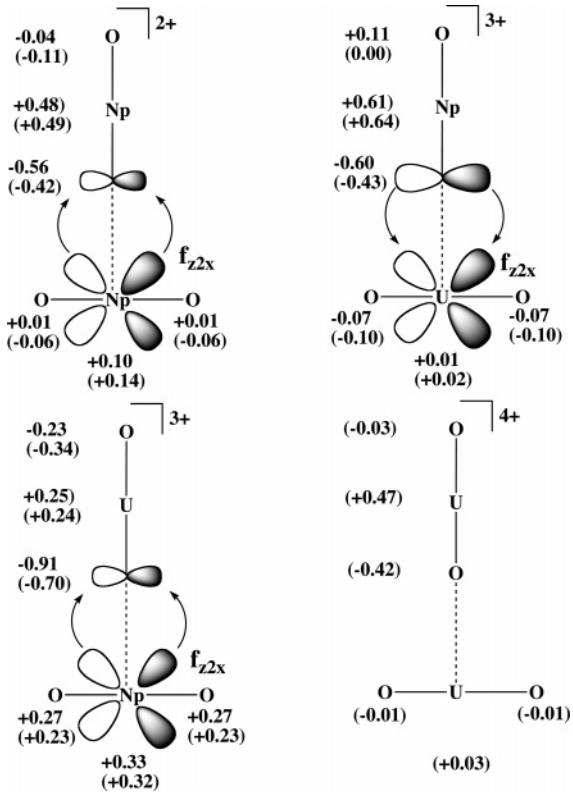

Figure 4. Change in charge (relative to actinyl cations) caused by the formation of a CCI. The dominant orbital interaction is also indicated.

Np═O bond (0.138 Å, gas phase; 0.095 Å, solution). When the roles of the two actinyl cations are reversed, the (OUO−ONpO)$^{3+}$ complex is formed (i.e., UO_2^{2+} is the ligand and Np the metal center). The actinyl cation UO_2^{2+} is a better Lewis acceptor than NpO_2^{+} because of its greater positive charge. As a result, charge is transferred from the metal center to the ligand (0.87 e^-, gas phase; 0.79 e^-, solution). Actually, most of the charge transfer occurs from the oxygens of NpO_2^{+} to the oxygens of UO_2^{2+}. The (ONpO−OUO)$^{3+}$ complex is 90.5 kcal/mol less stable than NpO_2^{+} + UO_2^{2+} in the gas phase but 37.0 kcal/mol more stable in solution. The (OUO−ONpO)$^{3+}$ complex is less stable than (ONpO−OUO)$^{3+}$ by 15.6 kcal/mol in the gas phase and 14.4 kcal/mol in solution. Because UO_2^{2+} is a better Lewis acid than NpO_2^{+}, a stronger complex results when NpO_2^{+} coordinates to the uranium center of UO_2^{2+}.

In the (OUO−OUO)$^{4+}$ complex, the gas-phase complex could not be located because of the increased intracomplex electrostatic repulsion. In solution, no net charge is transferred between actinyl cation units. One of the U═O bonds of the actinyl cation ligand has elongated and polarized. The (OUO−OUO)$^{4+}$ complex is 5.3 kcal/mol less stable than two UO_2^{2+} units in solution. The (ONpO−ONpO)$^{2+}$ and (ONpO−

(61) (a) Allen, P. G.; Bucher, J. J.; Shuh, D. K.; Edelstein, N. M.; Reich, T. *Inorg. Chem.* **1997**, *36*, 4676. (b) Gaillard, C.; El Azzi, A.; Billard, I.; Bolvin, H.; Hennig, C. *Inorg. Chem.* **2005**, *44*, 852.

(62) For alternative XAFS measurements on UO_2^{2+} and NpO_2^{+}, see: (a) Wahlgren, U.; Moll, H.; Grenthe, I.; Schimmelpfenning, B.; Maron, L.; Vallet, V.; Gropen, O. *J. Phys. Chem. A* **1999**, *103*, 8257. (b) Combes, J.-M.; Chisholm-Brause, C. J.; Brown, G. E., Jr.; Parks, G. A.; Conradson, S. D.; Eller, P. G.; Triay, I. R.; Hobart, D. E.; Meijer, A. *Environ. Sci. Technol.* **1992**, *26*, 376.

$OUO)^{3+}$ complexes are predicted to exist in solution, while $(OUO-OUO)^{4+}$ is not predicted to exist. These predictions are in accordance with observations. Solvation effects on $(ONpO-ONpO)^{2+}$ and $(ONpO-OUO)^{3+}$ binding are greater than 100 kcal/mol. Solvation is predicted to increase the binding free energy of $(OUO-OUO)^{4+}$ by 301.3 kcal/mol, an amount which is not sufficient to overcome electrostatic repulsion.

Grigoriev et al.[8] observed that no CCIs were present in the precipitates of a NpO_2ClO_4 solution with urea, which suggested that urea was a better ligand than water or NpO_2^+. This suggests that it may be reasonable to consider NpO_2^+ as a ligand with a binding similar to water but less than urea.

Conclusion

While CCIs have been known for 40 years, a theoretical study of the interactions has not been reported. The solution-phase complexes of $(ONpO-ONpO)^{2+}$, $(ONpO-OUO)^{3+}$, and $(OUO-OUO)^{4+}$ all have a T-shaped structure where the oxygen of one actinyl unit coordinates to the metal of the other unit. In the gas phase, all actinyl−actinyl complexes are much less stable than separated actinyl cations. Because of the quadratic dependence of charge on solvation, the complexes are significantly stabilized in solution. The complexes of $(ONpO-ONpO)^{2+}$ and $(ONpO-OUO)^{3+}$ are predicted to bind spontaneously in solution ($\Delta G = -42.1$ and -29.2 kcal/mol, respectively), while $(OUO-OUO)^{4+}$ is not predicted to form ($\Delta G = 13.2$ kcal/mol). These calculations are in accordance with experimental observations.

Acknowledgment. Computer time was made available on the Auburn COSAM PRISM cluster and by The Netherlands National Center for Computing Facilities (SARA). M.L.M. acknowledges computational support from the MSCF Computational Grand-Challenge Grant "Reliable Relativistic Quantum Chemistry Calculations for Molecules with Heavy Elements".

Supporting Information Available: Cartesian coordinates of all BPW91/TZ2P-optimized structures in Table 1 in the gas phase and in solution (COSMO optimization) and all B3LYP/LANL2DZ-optimized structures in Table 3 are presented in Table S1. This material is available free of charge via the Internet at http://pubs.acs.org.

IC050224O